

---

# GENETIC ALGORITHM WITH A BAYESIAN APPROACH FOR THE DETECTION OF MULTIPLE POINTS OF CHANGE OF TIME SERIES OF COUNTING EXCEEDANCES OF SPECIFIC THRESHOLDS

---

**Biviana Marcela Suárez-Sierra**

Computing and analytics area. School of Applied Sciences and Engineering.  
EAFIT University  
Medellín, Colombia  
bmsuarezs@eafit.edu.co

**Arrigo Coen**

Department of Mathematics, Faculty of Sciences.  
National Autonomous University of México  
CDMX, México, México  
coen@ciencias.unam.mx

**Carlos Alberto Taimal**

Computing and analytics area. School of Applied Sciences and Engineering.  
EAFIT University  
Medellín, Colombia  
cataimaly@eafit.edu.co

## ABSTRACT

The change-point detection problem has been widely studied in time series and signal processing literature. The current methods can be resumed in the search for the appropriate partitions of a whole time series such that the problem can be approached as one of optimization; nevertheless, an exact optimization approach could result computationally expensive and approximate ones discard potential scenarios for change-points configurations in a non-rigorous manner. Thus, a framework it is presented to detect change-points in a univariate time series using a decision criterion based on the Minimum Description Length (*MDL*), modified such that a Bayesian analysis is included. To search for the points of change, the times where mean value deviations occur (exceedances) are analyzed and then it is evaluated which of these could constitute a change-point through a genetic algorithm using as a fitness function the previously described *MDL*. The effectiveness of the method it is assessed through a simulation study and on the other hand, it is analyzed its practical validity in a real dataset for the presence of Particulate Matter of less than 2.5 microns ( $\mu m$ )  $PM_{2.5}$  in Bogotá, Colombia for the 2018-2020 period under different settings to understand the algorithm convergence. It is found that this definition for the objective function tends to find better results for both the number of change-points and their location in the series for most of cases reducing the error in comparison to other available methods in the literature.

**Keywords** Multiple Change-point Detection · Genetic Algorithms · Minimum Description Length · Non-homogeneous Poisson Processes · Maximum A Posteriori Estimation

## 1 Introduction

The change-point analysis problem has been widely covered in the time series and signal processing literature [1, 2]. A change in a time series or signal is defined as a deviation from the normal behaviour in reference to a parameter

or feature of the generating process of interest, and, consequently, a change-point is defined as the time where such deviation occurs. Some of these shifts include but are not limited to changes in the mean, variance or standard deviation, location and scale parameters and in general, any parameter of the assumed generating process to mention a few.

Now as there are multiple scenarios that determine a change and its respective time, also there are multiple methodologies available to finding them. Two exhaustive surveys are found in the works of [3, 2] to which the reader is referred to for a detailed review on the subject. From the second work it is noteworthy the typology used to describe change-point detection algorithms that are expressed as an optimization problem composed of an objective function, a search method, and a penalty on the analyzed parameters. Thus, the aim of a change-point detection algorithm is to segment a time series according to an optimality criterion which generally corresponds to a value that maximizes a penalized likelihood function.

On the other hand, to find the total of change-points and their location a method to search the solution space is used. Nevertheless, as the problem's complexity increases when the time series granularity does it as well, the use of exact methods implies a high computation cost. For example, a method used by [4] based on dynamic programming had a time complexity of  $O(T^2)$  with  $T$  the length of the series. Likewise, considering  $J$  as the total of change-points, there are  $\binom{T}{J}$  possible settings to evaluate and, if it was decided to compute the objective function value for all of them, i.e., for  $J = 0, 1, 2, \dots, T$ , there would be  $2^T$  scenarios to analyze [5].

Thus, and based on the work of [6, 5, 7, 8] is presented a method which uses a genetic algorithm as a search method modifying the objective function such that a Bayesian analysis is included and the Maximum A Posteriori estimation (MAP) function is used instead of the Maximum Likelihood one. On the other hand, we did not considered the underlying distribution for the observed data but the times where deviations from the mean or exceedances did occur, methodology adapted from Survival Analysis overcoming the need of a prior parametric definition for the generating process.

The rest of this paper is organized as follows: section (2) presents the inferential analysis corresponding to the existence of exceedances from the mean of the process, modeled using the rate and intensity functions of a non-homogeneous Poisson process for the times; in the subsections of this, (2.1) and (2.2) is presented the proposal for detecting such exceedances, using a genetic algorithm to search for these points and using as an objective function a modified version of the Minimum Description Length (MDL) principle. Next, in section (3), the derivation for the objective function are exposed for each one of the considered intensity functions such that in section (4) the performance of the algorithm is assessed through simulated and real data. Finally in section (5) the conclusions in regards of the found results are presented.

## 2 Inferential Analysis of the Univariate Non-Homogeneous Poisson Process

Based on the construction of the likelihood from a non-homogeneous Poisson process discussed in [9] and [10], we have the following expression, from which we will start to construct the penalized MAP function. The developments that will be shown in the following sections will be based on the assumption that some of the functions of the expression 1 correspond to the intensity function of the Non-homogeneous Poisson Process (NHPP).

$$\begin{aligned} \lambda^{(W)}(t|\theta) &= (\alpha/\beta)(t/\beta)^{\alpha-1}, & \alpha, \beta > 0 \\ \lambda^{(MO)}(t|\theta) &= \frac{\beta}{t+\alpha}, & \alpha, \beta > 0 \\ \lambda^{(GO)}(t|\theta) &= \alpha\beta \exp(-\beta t), & \alpha, \beta > 0 \\ \lambda^{(GGO)}(t|\theta) &= \alpha\beta\gamma t^{\gamma-1} \exp(-\beta t^\gamma), & \alpha, \beta, \gamma > 0. \end{aligned} \tag{1}$$

Each letter in the superscript of the left-hand term corresponds to the initial letter of the name of the distribution used as intensity function as follows, Weibull ( $W$ ) [11, 12], Musa-Okumoto ( $MO$ ) [13], Goel-Okumoto ( $GO$ ) and a generalization of the Goel-Okumoto model ( $GGO$ ) [14], for which the cumulative average function,  $m(t|\theta)$  is defined respectively by:

$$\begin{aligned} m^{(W)}(t|\theta) &= (t/\beta)^\alpha, & \alpha, \beta > 0 \\ m^{(MO)}(t|\theta) &= \beta \log\left(1 + \frac{t}{\alpha}\right), & \alpha, \beta > 0 \\ m^{(GO)}(t|\theta) &= \alpha[1 - \exp(-\beta t)], & \alpha, \beta > 0 \\ m^{(GGO)}(t|\theta) &= \alpha[1 - \exp(-\beta t^\gamma)], & \alpha, \beta, \gamma > 0. \end{aligned} \tag{2}$$

In the first three cases, the vector of parameters is  $\theta = (\alpha, \beta)$  and for the last one  $\theta = (\alpha, \beta, \gamma)$ .

## 2.1 Likelihood function with change points

A change point is defined as an instant where the structural pattern of a time series shifts. We assumed the presence of  $J$  change-points,  $\{\tau_1, \tau_2, \dots, \tau_J\}$  such that there are variations on the model parameters in between segments  $\tau_{j-1} < t < \tau_j, j = 0, 1, 2, \dots, J+1, j_0 = 1, j_{J+1} = T$ . These changes can be attributed to environmental policies or legislations in a certain year, the suspension of some network station due to maintenance for a climate case, macroeconomic policies from an economic standpoint or the presence of an stimulus in a neuroscience context. Then, the intensity functions of the NHPP have the form,

$$\lambda(t|\theta) = \begin{cases} \lambda(t|\theta_1), & 0 \leq t < \tau_1, \\ \lambda(t|\theta_j), & \tau_{j-1} \leq t < \tau_j, \quad j = 2, 3, \dots, J, \\ \lambda(t|\theta_{J+1}), & \tau_J \leq t \leq T, \end{cases} \quad (3)$$

where  $\theta_j$  is the vector of parameters between the change points  $\tau_{j-1}$  and  $\tau_j$ , for  $j = 2, \dots, J$ , and  $\theta_1$  and  $\theta_{J+1}$  are the parameter vectors before and after the first and last change points, respectively. With  $n$  observations, the functions for the means are (see, e.g., [15]),

$$m(t|\theta) = \begin{cases} m(t|\theta_1), & 0 \leq t < \tau_1, \\ m(\tau_1|\theta_1) + m(t|\theta_2) - m(\tau_1|\theta_2), & \tau_1 \leq t < \tau_2, \\ m(t|\theta_{j+1}) - m(\tau_j|\theta_{j+1}) \\ + \sum_{i=2}^j [m(\tau_i|\theta_i) - m(\tau_{i-1}|\theta_i)] \\ + m(\tau_1|\theta_1), & \tau_j \leq t < \tau_{j+1}, \quad j = 2, 3, \dots, J, \end{cases} \quad (4)$$

where  $\tau_{J+1} = T$ . That is, because  $m(t|\theta_1)$  represents the average number of exceedances of the standard, before the first change point.  $m(\tau_1|\theta_1) + m(t|\theta_2) - m(\tau_1|\theta_2)$  is the average number of exceedances of the standard between the first change point  $\tau_1$  and the second one  $\tau_2$ , given that the vector of parameters  $\theta_2$  is known, and so on.

Be  $D = d_1, \dots, d_n$ , where  $d_k$  (as in the case without change points), is the time of occurrence of the  $k$ th event (the  $k$ th time the maximum level of the environmental standard is exceeded), with  $k = 1, 2, \dots, n$ , the likelihood function is determined by the expression below where  $N_{\tau_i}$  represents the number of exceedances before the change point  $\tau_i$ , with  $i = 1, 2, \dots, J$  (see [16, 17]).

$$\begin{aligned} L(\mathbf{D}|\phi) &\propto \left[ \prod_{i=1}^{N_{\tau_1}} \lambda(d_i | \theta_1) \right] e^{-m(\tau_1|\theta_1)} \\ &\times \left[ \prod_{j=2}^J \left( \prod_{i=N_{\tau_{j-1}}+1}^{N_{\tau_j}} \lambda(d_i | \theta_j) \right) e^{-[m(\tau_j|\theta_j) - m(\tau_{j-1}|\theta_j)]} \right] \\ &\times \left[ \prod_{i=N_{\tau_J}+1}^n \lambda(d_i | \theta_{J+1}) \right] e^{-[m(T|\theta_{J+1}) - m(\tau_J|\theta_{J+1})]}, \end{aligned} \quad (5)$$

Using the expression (5), we infer the parameters  $\phi = (\theta, \tau)$ , with  $\theta = (\theta_1, \dots, \theta_J)$  and  $\tau = (\tau_1, \dots, \tau_J)$  using a Bayesian approach. This perspective consists of finding the relationship between the a priori distribution of the parameter  $\theta$ , on whose intensity function  $\lambda(t|\theta)$  is dependent and the a posteriori distribution of the same, after taking into consideration the observed information  $D$ . In [18], this method was applied to obtained results very close to the observed ones, hence the descriptive capacity of the model and the methodology used. In such work, the criteria used to select the model that best fits the data together with the graphic part was the MDL.

## 2.2 Detection of multiple change points using genetic algorithm

### 2.2.1 MDL framework

Since finding  $J$  change-points implies finding out  $J + 1$  regimes for the time series or fitting  $J + 1$  models with different parameters, statistical criteria has been used for such purpose in the available literature. Some include the Akaike Information Criterion (AIC), the Bayesian Information Criterion (BIC), Cross-Validation methods, and MDL-based methods. For problems involving regime shift detection, MDL methods usually provide superior empirical results. This superiority is probably due to the fact that both AIC and BIC apply the same penalty to all parameters, regardless of the nature of the parameter. On the other hand, MDL methods can adapt penalties to parameters depending on their nature be it continuous or discrete, bounded or not. In short, MDL defines the best fitting model as the one that enables the best compression of the data minimizing a penalized likelihood function. That is,

$$MDL = -\log_2(L_{opt}) + P. \quad (6)$$

Here  $\log_2(L_{opt})$  is the required amount of information needed to store the fitted model, term taken from information theory. More details on this can be found in [19].  $L_{opt}$  is obtained from replacing the maximum likelihood estimator in the likelihood function (5). This will be explained in more detail in the next section.

Because of the above, it is possible to make the natural connection between the likelihood and the MDL objective function by means of the penalty  $P$  (see [19]). The broad penalty methodology is summarized in three principles as stated by [5]. The first one is to penalize the real valued parameters by the number of observations. Say  $k$  that are used to estimate it, then, the penalty will be  $\frac{\log_2 k}{2}$ . For this principle, it is important to take into consideration how the observations are arranged to calculate the parameter of interest because this arrangement will be reflected in the penalty.

The second principle involves the penalty of how many integer parameters, such as the number of change points  $J$  and where they are located represented by  $\tau_1, \dots, \tau_J$  should be charged. This charging is calculated based on the value for each of them. For example, the quantity  $J$ , which is bounded by the total number of observations  $T$  is charged an amount of  $\frac{\log_2 T}{2}$ . For each of the  $\tau_j$  with  $j = 1, \dots, J$ , we have that  $\tau_j < \tau_{j+1}$ , therefore the cost of its penalty will be  $\frac{\log_2 \tau_{j+1}}{2}$  for  $j = 2, \dots, J$ .

The last principle, mentioned in [5], is the additivity principle. It involves constructing  $P$  based on the sum of all the partial penalties mentioned above. The more parameters the model has, the higher  $P$  will be. However, if despite adding parameters, the expression  $\log_2(L_{opt})$  does not grow larger than the penalty  $P$  of the extra parameters, the simpler model will be preferred. For the purposes of this paper, the following will be used as the penalty function  $P_\tau(\theta)$  for a fixed change point configuration,

$$P_\tau(\theta) = R \sum_{j=1}^{J+1} \frac{\ln(\tau_j - \tau_{j-1})}{2} + \ln(J) + \sum_{j=2}^J \ln(\tau_j), \quad (7)$$

where  $R = 2, 3$  depending on whether  $\theta = (\alpha, \beta)$  or  $\theta = (\alpha, \beta, \gamma)$ , i.e. if  $\theta$  has one or two parameters. The first summand of the right-hand term of expression represents that each of the real-valued parameters  $(\alpha_j, \beta_j, \gamma_j)$  will be penalized by  $\frac{\ln(\tau_j - \tau_{j-1})}{2}$  of the  $j$ -th regime to which they belong and since there are  $J + 1$  regimes, the sum goes from 1 to  $J + 1$ . The second summand of the right-hand term is derived from the penalty of the number of points of change, and the last term comes from the sum of each of the penalties of each of the change points.

### 2.2.2 Genetic Algorithm Schema

As exposed in [5] the total possible cases to evaluate the MDL corresponds to  $\binom{T}{J}$ , where  $T$  is the number of observations in the time series and  $J$  is the number of change points. However, this number of parametric configurations is a quantity that does not make a computationally efficient optimization algorithm that aims to choose the best of the parametric configurations that minimize the MDL. For this reason, we will use the genetic algorithm that, by natural selection criteria will establish the best of the parameters configurations that we will call chromosomes. Each chromosome will be labeled as  $(J, \tau_1, \dots, \tau_J)$ , where the first component  $J$  stands for the number of change points,

located respectively at times  $\tau_1, \dots, \tau_J$ , corresponding to the respective coordinates. The following is to establish how the genetic algorithm (GA) evaluates each of the chromosomes, while avoiding those with a low probability of being optimal.

Let us now see how a complete generation is produced from an initial one with a given size, although the size can also be a couple. For this purpose, suppose there are  $k$  individuals or chromosomes in the initial generation set at random. Each of the  $T$  observations in the time series is allowed to be a change-point, independent of all other change-points, with probability, for example as seen in [5], of 0.06. The number of change points for each chromosome in the initial generation has a binomial distribution with parameters  $T - 1$  and 0.06, respectively.

Two chromosomes are taken out of the initial generation, one mother and one father chromosome, to make a child of the next generation. This is done by a probabilistic combination of the parents. The principle of natural selection in this context will be performed by selecting a pair of chromosomes that best optimize the expression (6) since this couple is considered to have the highest probability of having offspring. Therefore, the chromosomes are arranged from the most likely to the least likely to have children, and each individual of the same generation is assigned a ranking, say  $S_i$ , being the ranking of the  $j$ th individual, with  $S_j = 1, \dots, k$ . If  $S_j = k$  then  $j$  is the individual that best fits the objective function (6). If  $S_j = 1$  then  $j$  is the individual that least well fits the objective function (6).

Once this ranking has been made for each of the chromosomes of the same generation, we proceed to establish the probability of selection using the following expression that simulates the principle of natural selection of the parents that will generate the next generation.

$$\frac{S_j}{\sum_{i=1}^k S_i} \quad (8)$$

The chromosome that has the highest probability of being selected from the  $k$  chromosomes, is chosen as the mother. Among the remaining  $(k - 1)$  chromosomes, the father is chosen under the same selection criteria as the mother. Suppose that the mother chromosome has  $m$  change points, located in some  $\tau_1, \dots, \tau_m$ , i.e. with the parameter configuration  $(m, \tau_1, \dots, \tau_m)$ . Similarly, suppose the father chromosome has the parametric configuration  $(n, \delta_1, \dots, \delta_n)$ . A child of these parents can arise simply by joining the two chromosomes, i.e., the child chromosome will initially have the following configuration,  $(m + n, \epsilon_1, \dots, \epsilon_{m+n})$ , where the  $m + n$  change-points contain the mother's  $m$  and the father's  $n$  change-points.

After this, we remove the duplicated change-points from the child  $(m + n, \epsilon_1, \dots, \epsilon_{m+n})$ . From this last configuration, we keep all or some change-points. For this, in [5] use the dynamics of flipping a coin for each change-point in the child configuration. If heads comes up, the change-point is left, otherwise it is removed. That is, a binomial distribution will be used with probability parameter  $1/2$  and number of trials, the length of the configuration of the child minus duplicities. All this with the aim that the offspring will keep traits of the parents, without being exact replicas.

Each point of change in the child chromosome, can undergo a mutation; a schema taken from [5] is that one of the following three alternatives may happen. We start by generating, with some random mechanism, the numbers  $-1, 0$  and  $1$  with respective probabilities  $0.4, 0.3, 0.4$ . If  $-1$  comes out, the change point is subtracted by one unit; if  $0$  comes out, it stays at the time it is at, and if  $1$  comes out, the current change point is added by one unit. Again, duplicates are eliminated. With this last procedure, we have finished the construction of Child 1. Child 2 up to  $k$  are generated in the same way as the previous one. New parents are selected if chromosomes are duplicated in the same generation with the previous parents.

The process of generation is repeated as many times as generations are to be obtained. In fact, one of the criteria for establishing the completion of the genetic algorithm is to fix the number of generations  $r$ . Another approach could be to reach the solution that minimizes the objective function. The objective function for we used was  $\ln P_\tau(\theta) - \ln f(D|\theta) - \ln f(\theta)$ , i.e.

$$\hat{\theta}_{MDL-BAYESIAN} = \operatorname{argmax}_{\theta, \tau} (\ln P_\tau(\theta) - \ln f_\tau(D|\theta) - \ln f_\tau(\theta)) \quad (9)$$

In other words,  $\hat{\theta}_{MDL-BAYESIAN}$  is the maximum argument of the objective function, in which case it will be the optimal solution to the problem of finding the best configuration of shift points and the respective parameters of the regimes they determine.

### 3 Methods and Models

We are particularly interested in the likelihood function of expression (9) in order to establish what we have called the corresponding Bayesian-MDL. Therefore, for any  $m(t, \theta)$  defined in expression (2) and its respective intensity function defined in (1), it follows that,

$$L(\mathbf{D}|\phi) \propto e^{-m(\tau_1|\theta_1)} \prod_{i=1}^{N_{\tau_1}} \lambda(d_i|\theta_1) \times \prod_{j=2}^J \left( e^{-[m(\tau_j|\theta_j) - m(\tau_{j-1}|\theta_j)]} \prod_{i=N_{\tau_{j-1}}+1}^{N_{\tau_j}} \lambda(d_i|\theta_j) \right) \times e^{-[m(T|\theta_{J+1}) - m(\tau_J|\theta_{J+1})]} \prod_{i=N_{\tau_J}+1}^n \lambda(d_i|\theta_{J+1}) \quad (10)$$

since the product with respect to  $i$  only affects the functions  $\lambda(t, \theta)$  in each of the different  $J + 1$  regimes determined by the  $J$  change points in the vector  $\tau = (\tau_1, \tau_2, \dots, \tau_J)$ . Using that for  $J$  change points,  $\tau_{J+1} := T$  where  $T$  is the number of daily measurements,  $\tau_0 = 0$ ,  $N_0 = 0$  y  $m(0|\theta) = 0$ , it follows that the expression (10) reduces to,

$$L(\mathbf{D}|\phi) \propto \prod_{j=1}^{J+1} \left( e^{-[m(\tau_j|\theta_j) - m(\tau_{j-1}|\theta_j)]} \prod_{i=N_{\tau_{j-1}}+1}^{N_{\tau_j}} \lambda(d_i|\theta_j) \right) \quad (11)$$

Taking the logarithm of (11) we have,

$$\begin{aligned} \log L(\mathbf{D}|\phi) &= \left( \sum_{j=1}^{J+1} m(\tau_{j-1}|\theta_j) - m(\tau_j|\theta_j) \right) + \left( \sum_{j=1}^{J+1} \sum_{i=N_{\tau_{j-1}}+1}^{N_{\tau_j}} \log \lambda(d_i|\theta_j) \right) \\ &= \sum_{j=1}^{J+1} \left( m(\tau_{j-1}|\theta_j) - m(\tau_j|\theta_j) + \sum_{i=N_{\tau_{j-1}}+1}^{N_{\tau_j}} \log \lambda(d_i|\theta_j) \right) \end{aligned} \quad (12)$$

Also, the Bayesian principle states that,

$$f(\theta|D) \propto L(D|\theta)f(\theta), \quad (13)$$

where  $L$  is the likelihood function depending on the observations  $D$ , given the parameter vector  $\theta$  and,  $f(\theta)$  the a priori function of the parameter vector  $\theta$ . Taking logarithm for (13) we have that,

$$\ln f(\theta|D) \propto \ln(L(D|\theta)) + \ln(f(\theta)) \quad (14)$$

From (14), we start by establishing the general form of the a priori joint function  $f(\theta) = f(\alpha, \beta, \tau_j)$  in the first three cases, and  $f(\theta) = f(\alpha, \beta, \gamma, \tau_j)$  in the last function  $m$  of the term (2).

#### 3.1 A priori distributions

If we take  $\alpha \sim \text{Gamma}(\phi_{11}, \phi_{12})$ , then,

$$f(\alpha) = \frac{\phi_{11}^{\phi_{12}}}{\Gamma(\phi_{12})} \alpha^{\phi_{12}-1} e^{-\phi_{11}\alpha}$$

After applying logarithm we obtain,

$$\begin{aligned}\log f(\alpha) &= \log \left( \frac{\phi_{11}^{\phi_{12}}}{\Gamma(\phi_{12})} \alpha^{\phi_{12}-1} e^{-\phi_{11}\alpha} \right) \\ &= \phi_{12} \log \phi_{11} - \log \Gamma(\phi_{12}) + (\phi_{12} - 1) \log \alpha - \phi_{11}\alpha \\ &\propto (\phi_{12} - 1) \log \alpha - \phi_{11}\alpha\end{aligned}\tag{15}$$

Similarly for  $\beta$ , if we take  $\beta \sim \text{Gamma}(\phi_{21}, \phi_{22})$ , then,

$$\log f(\beta) \propto (\phi_{22} - 1) \log \beta - \phi_{21}\beta\tag{16}$$

On the other hand, assuming every time in the series can be chosen as a change-point  $\tau_j$  with the same probability, thus  $\tau_j \sim \text{Uniform}(0, T)$ ,  $j = 1, 2, \dots, J$ .

Then we have,

$$f(\tau_j) = \frac{1}{T}\tag{17}$$

Taking logarithm we obtain,

$$\log f(\tau_j) = -\log(T)\tag{18}$$

Rebuilding the joint function for  $\theta = (\alpha, \beta, \tau_j)$ , under the assumption of independence, we have,

$$\log f(\alpha, \beta, \tau_j) \propto (\phi_{12} - 1) \log \alpha - \phi_{11}\alpha + (\phi_{22} - 1) \log \beta - \phi_{21}\beta - \log(T)\tag{19}$$

In the three-parameter model for the intensity function, we have that, under the assumption of independence and that all the parameters have an a priori gamma distribution; considering also, the distribution for the change-points, thus we have,

$$\log f(\alpha, \beta, \gamma, \tau_j) = -\alpha\phi_{11} + (\phi_{12} - 1) \log \alpha - \beta\phi_{21} + (\phi_{22} - 1) \log \beta - \gamma\phi_{31} + (\phi_{32} - 1) \log \gamma - \log(T).\tag{20}$$

Up to this point, the second summand of the right-hand side of (14) has been obtained. Next, the first summand of the right-hand side of (14) will be derived, but this will be done depending on the intensity function of the non-homogeneous Poisson process that was established previously and whose cumulative mean functions are expressed in the four possibilities of (2).

### 3.1.1 Weibull intensity rate (W)

After taking the expressions for the intensity function  $\lambda^{(W)}(t|\theta)$  and the cumulative mean function  $m^{(W)}(t|\theta)$  using (2) and (1) respectively, and replacing these in (12) we have,

$$\begin{aligned}
 \log L(D|\phi) &= \sum_{j=1}^{J+1} \left( m(\tau_{j-1}|\theta_j) - m(\tau_j|\theta_j) + \sum_{i=N_{\tau_{j-1}}+1}^{N_{\tau_j}} \log \lambda(d_i|\theta_j) \right) \\
 &= \sum_{j=1}^{J+1} \left( \left( \frac{\tau_{j-1}}{\beta_j} \right)^{\alpha_j} - \left( \frac{\tau_j}{\beta_j} \right)^{\alpha_j} + \sum_{i=N_{\tau_{j-1}}+1}^{N_{\tau_j}} \log \left( \frac{\alpha_j}{\beta_j} \left( \frac{d_i}{\beta_j} \right)^{\alpha_j-1} \right) \right) \\
 &= \sum_{j=1}^{J+1} \left( \frac{\tau_{j-1}^{\alpha_j} - \tau_j^{\alpha_j}}{\beta_j^{\alpha_j}} + (N_{\tau_j} - N_{\tau_{j-1}}) (\log(\alpha_j) - \alpha_j \log(\beta_j)) \right. \\
 &\quad \left. + (\alpha_j - 1) \sum_{i=N_{\tau_{j-1}}+1}^{N_{\tau_j}} \log(d_i) \right) \tag{21}
 \end{aligned}$$

Substituting the expressions (7), (19), (21) in the objective function of the expression (9) we have that,

$$\begin{aligned}
 \ln P_\tau(\theta) - \ln f_\tau(D|\theta) - \ln f_\tau(\theta) &= 2 \sum_{i=1}^{J+1} \frac{\ln(\tau_i - \tau_{i-1})}{2} + \ln(J) + \sum_{i=2}^J \ln(\tau_i) \\
 &\quad - \sum_{j=1}^{J+1} \left( \frac{\tau_{j-1}^{\alpha_j} - \tau_j^{\alpha_j}}{\beta_j^{\alpha_j}} + (N_{\tau_j} - N_{\tau_{j-1}}) (\ln(\alpha_j) - \alpha_j \ln(\beta_j)) \right. \\
 &\quad \left. + (\alpha_j - 1) \sum_{i=N_{\tau_{j-1}}+1}^{N_{\tau_j}} \ln(d_i) \right) \\
 &\quad - \sum_{j=1}^{J+1} ((\phi_{12} - 1) \ln \alpha_j - \phi_{11} \alpha_j + (\phi_{22} - 1) \ln \beta_j - \phi_{21} \beta_j) + J \ln(T) \tag{22}
 \end{aligned}$$

### 3.1.2 Musa-Okumoto (MO)

Likewise, taking the expressions for the intensity function  $\lambda^{(MO)}(t|\theta)$  and the cumulative mean function  $m^{(MO)}(t|\theta)$  from (2) and (1) respectively, and replacing these values in (12) we have,

$$\begin{aligned}
 \log L(D|\phi) &= \sum_{j=1}^{J+1} \left( m(\tau_{j-1}|\theta_j) - m(\tau_j|\theta_j) + \sum_{i=N_{\tau_{j-1}}+1}^{N_{\tau_j}} \log \lambda(d_i|\theta_j) \right) \\
 &= \sum_{j=1}^{J+1} \left( \beta_j \log \left( \frac{\alpha_j + \tau_{j-1}}{\alpha_j} \right) - \beta_j \log \left( \frac{\alpha_j + \tau_j}{\alpha_j} \right) + \sum_{i=N_{\tau_{j-1}}+1}^{N_{\tau_j}} \log \left( \frac{\beta_j}{\alpha_j + d_i} \right) \right) \\
 &= \sum_{j=1}^{J+1} \left( \beta_j \log \left( \frac{\alpha_j + \tau_{j-1}}{\alpha_j} \right) - \beta_j \log \left( \frac{\alpha_j + \tau_j}{\alpha_j} \right) + (N_{\tau_j} - N_{\tau_{j-1}}) \log(\beta_j) - \sum_{i=N_{\tau_{j-1}}+1}^{N_{\tau_j}} \log(\alpha_j + d_i) \right) \\
 &= \sum_{j=1}^{J+1} \left( \beta_j (\log(\alpha_j + \tau_{j-1}) - \log(\alpha_j + \tau_j)) + (N_{\tau_j} - N_{\tau_{j-1}}) \log(\beta_j) - \sum_{i=N_{\tau_{j-1}}+1}^{N_{\tau_j}} \log(\alpha_j + d_i) \right) \tag{23}
 \end{aligned}$$

Now, after replacing (7), (23), and (19) in (9) we have,



$$\begin{aligned}
P_\tau(\theta) - \ln f_\tau(D|\theta) - \ln f_\tau(\theta) &= 2 \sum_{i=1}^{J+1} \frac{\ln(\tau_i - \tau_{i-1})}{2} + \ln(J) + \sum_{i=2}^J \ln(\tau_i) \\
&\quad - \sum_{j=1}^{J+1} \left( \beta_j (\ln(\alpha_j + \tau_{j-1}) - \ln(\alpha_j + \tau_j)) + (N_{\tau_j} - N_{\tau_{j-1}}) \ln(\beta_j) \right. \\
&\quad \left. - \sum_{i=N_{\tau_{j-1}}+1}^{N_{\tau_j}} \ln(\alpha_j + d_i) \right) \\
&\quad - \sum_{j=1}^{J+1} ((\phi_{12} - 1) \ln \alpha_j - \phi_{11} \alpha_j + (\phi_{22} - 1) \ln \beta_j - \phi_{21} \beta_j) + J \ln(T)
\end{aligned} \tag{24}$$

### 3.1.3 Goel-Okumoto (GO)

As for the previous cases, we take the expressions  $\lambda^{(GO)}(t|\theta)$  and  $m^{(GO)}(t|\theta)$  from (2) and (1) respectively, and replace this values in (12). Then we have,

$$\begin{aligned}
\log L(D|\phi) &= \sum_{j=1}^{J+1} \left( m(\tau_{j-1}|\theta_j) - m(\tau_j|\theta_j) + \sum_{i=N_{\tau_{j-1}}+1}^{N_{\tau_j}} \log \lambda(d_i|\theta_j) \right) \\
&= \sum_{j=1}^{J+1} \left( \alpha_j [1 - e^{-\beta_j \tau_{j-1}}] - \alpha_j [1 - e^{-\beta_j \tau_j}] + \sum_{i=N_{\tau_{j-1}}+1}^{N_{\tau_j}} \log(\alpha \beta e^{-\beta d_i}) \right) \\
&= \sum_{j=1}^{J+1} \left( \alpha_j [e^{-\beta_j \tau_j} - e^{-\beta_j \tau_{j-1}}] + (N_{\tau_j} - N_{\tau_{j-1}}) \log(\alpha \beta) - \beta \sum_{i=N_{\tau_{j-1}}+1}^{N_{\tau_j}} d_i \right)
\end{aligned} \tag{25}$$

Replacing the expressions (7), (25), (19) in the objective function of the expression (9) we have that

$$\begin{aligned}
P_\tau(\theta) - \ln f_\tau(D|\theta) - \ln f_\tau(\theta) &= 2 \sum_{i=1}^{J+1} \frac{\ln(\tau_i - \tau_{i-1})}{2} + \ln(J) + \sum_{i=2}^J \ln(\tau_i) \\
&\quad - \sum_{j=1}^{J+1} \left( \alpha_j [e^{-\beta_j \tau_j} - e^{-\beta_j \tau_{j-1}}] + (N_{\tau_j} - N_{\tau_{j-1}}) \ln(\alpha \beta) - \beta \sum_{i=N_{\tau_{j-1}}+1}^{N_{\tau_j}} d_i \right) \\
&\quad - \sum_{j=1}^{J+1} ((\phi_{12} - 1) \ln \alpha_j - \phi_{11} \alpha_j + (\phi_{22} - 1) \ln \beta_j - \phi_{21} \beta_j) + J \ln(T)
\end{aligned} \tag{26}$$

### 3.1.4 Generalized Goel-Okumoto (GGO)

Finally and once again, we take  $\lambda^{(GGO)}(t|\theta)$  and  $m^{(GGO)}(t|\theta)$  from (2) and (1) respectively, and replace these values in (12) and then,

$$\begin{aligned}
\log L(D|\phi) &= \sum_{j=1}^{J+1} \left( m(\tau_{j-1}|\theta_j) - m(\tau_j|\theta_j) + \sum_{i=N_{\tau_{j-1}}+1}^{N_{\tau_j}} \log \lambda(d_i|\theta_j) \right) \\
&= \sum_{j=1}^{J+1} \left( \alpha_j \left( 1 - e^{-\beta_j \tau_{j-1}^{\gamma_j}} \right) - \alpha_j \left( 1 - e^{-\beta_j \tau_j^{\gamma_j}} \right) + \sum_{i=N_{\tau_{j-1}}+1}^{N_{\tau_j}} \ln \left( \alpha_j \beta_j \gamma_j d_i^{\gamma_j-1} e^{-\beta_j d_i^{\gamma_j}} \right) \right) \\
&= \sum_{j=1}^{J+1} \left( \alpha_j \left( e^{-\beta_j \tau_j^{\gamma_j}} - e^{-\beta_j \tau_{j-1}^{\gamma_j}} \right) + (N_{\tau_j} - N_{\tau_{j-1}}) \ln(\alpha_j \beta_j \gamma_j) \right. \\
&\quad \left. + (\gamma_j - 1) \left( \sum_{i=N_{\tau_{j-1}}+1}^{N_{\tau_j}} \ln d_i \right) - \beta_j \left( \sum_{i=N_{\tau_{j-1}}+1}^{N_{\tau_j}} d_i^{\gamma_j} \right) \right) \tag{27}
\end{aligned}$$

Substituting (7), (27), and (20) in (9) we have,

$$\begin{aligned}
P_\tau(\theta) - \ln f_\tau(D|\theta) - \ln f_\tau(\theta) &= 3 \sum_{i=1}^{J+1} \frac{\ln(\tau_i - \tau_{i-1})}{2} + \ln(J) + \sum_{i=2}^J \ln(\tau_i) \\
&\quad - \sum_{j=1}^{J+1} \left( \alpha_j \left( e^{-\beta_j \tau_j^{\gamma_j}} - e^{-\beta_j \tau_{j-1}^{\gamma_j}} \right) + (N_{\tau_j} - N_{\tau_{j-1}}) \ln(\alpha_j \beta_j \gamma_j) \right. \\
&\quad \left. + (\gamma_j - 1) \left( \sum_{i=N_{\tau_{j-1}}+1}^{N_{\tau_j}} \ln d_i \right) - \beta_j \left( \sum_{i=N_{\tau_{j-1}}+1}^{N_{\tau_j}} d_i^{\gamma_j} \right) \right) \\
&\quad - \sum_{j=1}^{J+1} (\alpha_j \phi_{11} + (\phi_{12} - 1) \ln(\alpha_j) - \beta_j \phi_{21} + (\phi_{22} - 1) \ln(\beta_j) \\
&\quad - \gamma_j \phi_{31} + (\phi_{32} - 1) \ln(\gamma_j)) + J \ln(T) \tag{28}
\end{aligned}$$

Therefore, the expressions (22), (24), (26) and (28) are the objective functions that by minimizing the Bayesian MDL is obtained for each of the different functions  $\lambda(t|\theta)$  of the expression (1), respectively.

Each of the members of the same generation will have a Bayesian-MDL, of which the smallest is chosen. This is done for all the generations. At the end, we will have as many Bayesian-MDLs as generations, and the minimum corresponding to the solution sought in the problem of determining the points of change of the time series of intervals is chosen.

## 4 Results and discussion

In this section, we proceed to asses the performance of the algorithm to detect multiple change-points. For this purpose we consider two datasets, the first one being simulated observations and the second one consistent of records of particulate matter of less than 2.5 microns of diameter ( $PM_{2.5}$ ) in the city of Bogotá, Colombia collected during the period 2018-2020 on a daily basis.

For the implemented experiments, only the Weibull mean cumulative function (23) was considered with optimal values for the parameters  $\alpha$  and  $\beta$ , 0.1 and 0.5 respectively, which were estimated via the `optim` function of the statistical software R [20]; on the other hand, for  $\alpha$  and  $\beta$  we used as a priori distributions  $Gamma(\phi_{i1}, \phi_{i2})$ ,  $i = 1, 2$  as we previously defined in section (3.1.1) and the optimal values for the hyperparameters were found to be  $\phi_{11} = 1$ ,  $\phi_{12} = 2$ ,  $\phi_{21} = 3$  and  $\phi_{22} = 1.2$  estimated using Markov-Chain Monte Carlo (MCMC) methods such that, the objective function takes the form of (21).

We start by analyzing the simulated data under different settings which will be described soon in a detailed manner and then we proceed with the real data. For this task we used the statistical software R; the scripts and datasets can be shared on reader's request.

#### 4.1 Simulation study

To assess the performance of the algorithm on simulated data, we proceed under a similar scheme as the one proposed by [5]. Three different cases were considered for the number of change-points  $J$ , 1, 2 and 3 and three different settings for their locations  $\tau_1, \tau_2, \dots, \tau_J$  were selected in a convenient manner to illustrate, such that these are presented in table (1).

Taking into account that the length of the  $PM_{2.5}$  series for Bogotá during the period 2018-2020, was 1096, such number of observations were simulated from a *log-normal* distribution with scale parameter  $\mu \in \mathcal{R}$  and of shape  $\sigma > 0$  (see expression (29)). The data was approximated to this distribution according to the results obtained through the library `fitdistrplus` [21] in R and the ones published by [22].

$$f(x) = \begin{cases} \frac{1}{x\sigma\sqrt{2\pi}} \exp\left(-\frac{(\ln(x)-\mu)^2}{2\sigma^2}\right), & x > 0 \\ 0, & x < 0 \end{cases} \quad (29)$$

Now, as  $J$  change-points split the time series into  $J + 1$  sub-series or regimes, for each  $J$  every regime was generated by incrementally varying the scale parameter  $\mu$  in 0.5 units while the parameter  $\sigma$  was held constant and equal to 0.32. Thus, the values of  $\mu$  and  $\sigma$  used to generate the  $J + 1$  regimes,  $J \in \{1, 2, 3\}$  are presented in table (2) while the series behavior for different settings of  $\tau_1, \tau_2, \dots, \tau_J$  can be appreciated in figure (1) such that the vertical dashed lines represent the change-points. On the other hand, again to illustrate, we defined as threshold for possible exceedances the arithmetic mean of the 1096 simulations,  $\bar{X} = \frac{1}{1096} \sum_{t=1}^{1096} X_t$ .

For each of the nine settings, the number of change-points were estimated, the optimal Bayesian-MDL and the cumulative mean function,  $m(t|\theta)$  and for every run of the genetic algorithm, 50 generations with 50 individuals each were used; the proportion of the times used to generate the initial population was of 6% and the mutation probability was 3% as in [5]. This results are presented and analyzed in the following section.

Number of Change-points	Setting	Locations
1	1	$\tau_1 = 548$
	2	$\tau_1 = 275$
	3	$\tau_1 = 825$
2	1	$\tau_1 = 275, \tau_2 = 821$
	2	$\tau_1 = 547, \tau_2 = 823$
	3	$\tau_1 = 365, \tau_2 = 730$
3	1	$\tau_1 = 275, \tau_2 = 549, \tau_3 = 823$
	2	$\tau_1 = 548, \tau_2 = 823, \tau_3 = 973$
	3	$\tau_1 = 169, \tau_2 = 413, \tau_3 = 1027$

Table 1: Different settings for change-points simulations

##### 4.1.1 One Change-point

###### First Setting

We start by analyzing the behavior of the genetic algorithm under the presence of one change-point. In this case, the change-point was  $\tau_1 = 548$ . In the upper left panel of figure (2), it can be found the mean cumulative function (black solid line) and the fitting by means of the Bayesian-MDL (solid red line in the middle), as well as the confidence intervals at 95% (solid blue lines). Around the time associated with  $\tau_1$  a break is experienced such that the values taken by  $m(t|\theta)$  until here increase in a steady manner reaching a local maximum there; after that instant a gradual growth is

Number of Change-points	Number of regimes	Distribution for each regime
1	2	$\log - normal(\mu = 3.5, \sigma = 0.32)$ , $\log - normal(\mu = 4.0, \sigma = 0.32)$
2	3	$\log - normal(\mu = 3.5, \sigma = 0.32)$ , $\log - normal(\mu = 4.0, \sigma = 0.32)$ , $\log - normal(\mu = 4.5, \sigma = 0.32)$
3	4	$\log - normal(\mu = 3.5, \sigma = 0.32)$ , $\log - normal(\mu = 4.0, \sigma = 0.32)$ , $\log - normal(\mu = 4.5, \sigma = 0.32)$ , $\log - normal(\mu = 5.0, \sigma = 0.32)$

Table 2: Settings for the time series regimes for different number of change-points

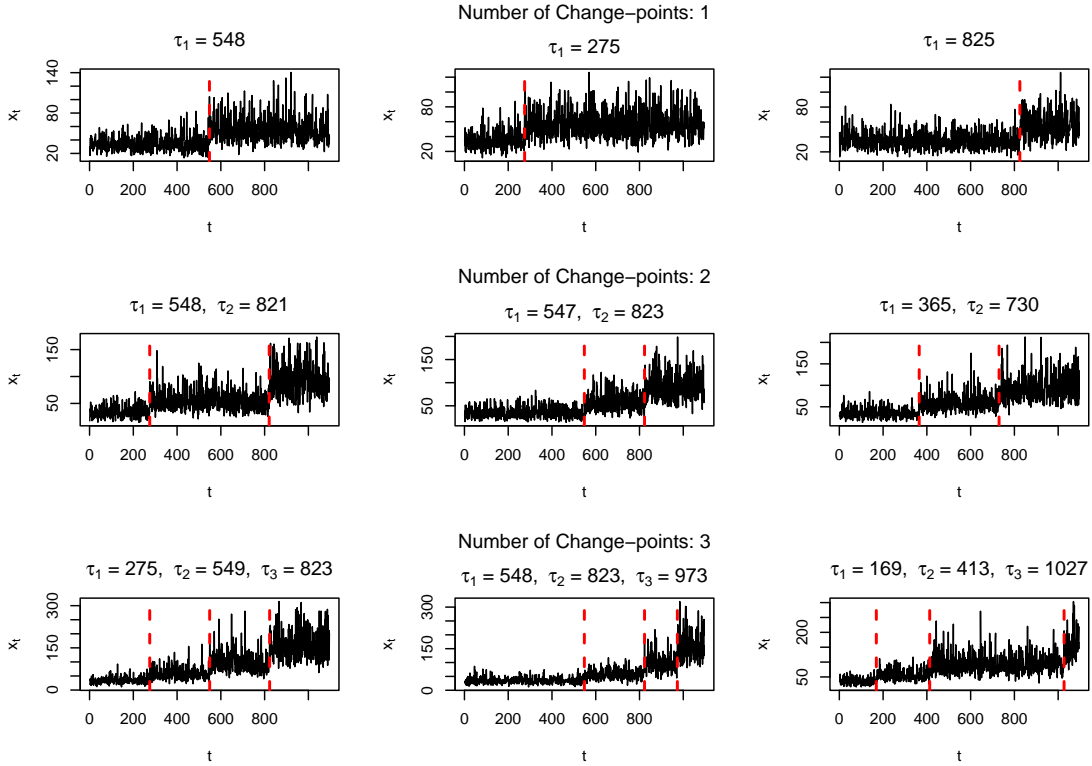


Figure 1: Simulated time series behavior

experienced until the end of the series.

On the other side in the upper right panel of figure (2) the evolution of the Bayesian-MDL is presented in terms of the iterations or generations of the genetic algorithm such that an optimum of just more than 800 is reached around of the 50th generation; this can be better appreciated in the lower right panel by a vertical dashed line while the horizontal dashed line points out the number of change-points detected as optimal which in this case was two.

While the number of change-points estimated was larger in one unit than the real one,  $J = 1$  the algorithm succeeds in capturing the behavior of such change-point as can be seen in the lower left panel such that the higher

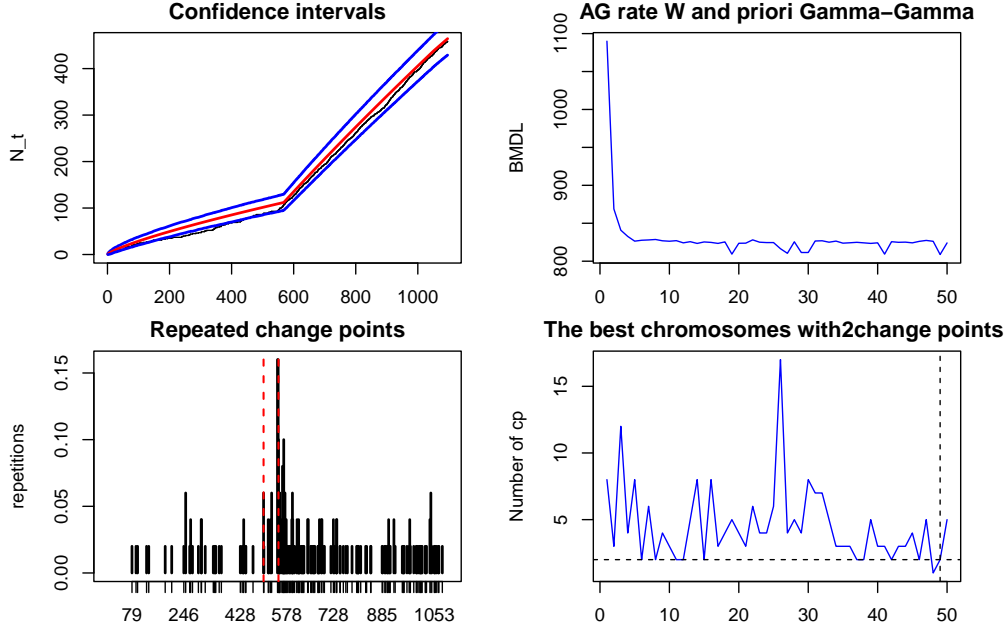


Figure 2: Genetic algorithm results - 1 change-point, first setting

frequency is reached around the time 548. Also if we define a neighborhood of six change-points detected before and after said instant (vertical dashed lines), in 50% of the time the detected change-points cluster around the real  $\tau_1$ .

## Second Setting

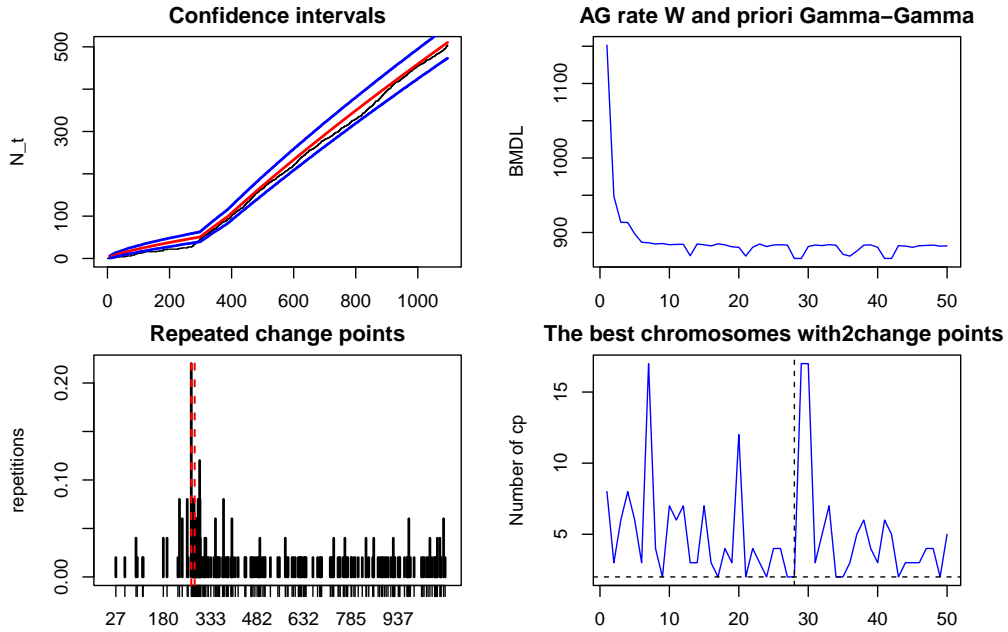


Figure 3: Genetic algorithm results - 1 change-point, second setting

Now we consider the second setting for the presence of one change-point,  $\tau_1 = 275$  the results of which are presented graphically in figure (3). Again with the optimal values estimated by the Bayesian-MDL the mean cumulative function  $m(t|\theta)$  is fitted as presented in the upper left panel (solid middle red line) with its respective 95% confidence interval (upper and lower solid blue lines); in an analogous manner to the previous setting around the time where a change is

experienced there is also a break in the values taken by the function, that is from time 1 until just before time 275 such that  $m(t|\theta)$  grows in a steady and monotonous manner and after this instant a more pronounced growth can be seen until reaching the end of the series.

On the other side, the next figure (upper right panel) presents the evolution of the Bayesian-MDL ( $y$  axis) for each generation of the genetic algorithm ( $x$  axis). The value detected as optimal for the objective function was found to be slightly under 900 and such was reached in generation 30 as indicated by the vertical dashed line in the lower right panel of figure (3); now, the number of change-points associated to such value was  $J = 2$  while the real value of  $J$  was equal to 1.

Despite the stated above in the lower left panel, again, a cluster can be found around the real value of the change-point  $\tau_1$  and furthermore, in approximately 50% of the generations such instant can be found in around a neighborhood of a week before and after its location.

### Third Setting

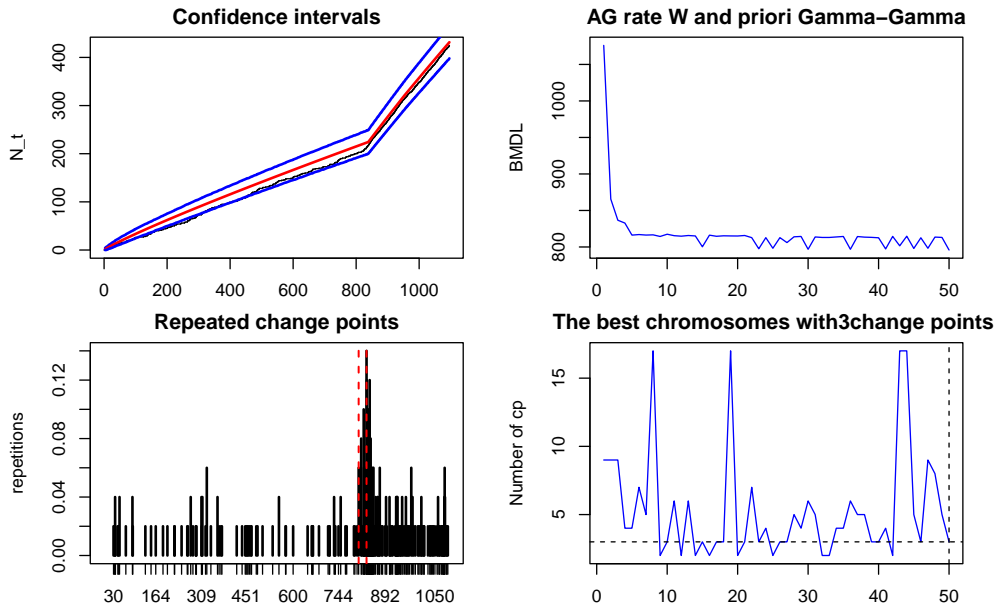


Figure 4: Genetic algorithm results - 1 change-point, third setting

Finally we consider the third setting for the presence of one change-point which was located at time 825, i.e.,  $\tau_1 = 825$ . The genetic algorithm was again implemented and the mean cumulative function was fitted, the Bayesian-MDL values were computed for each generation and as well the optimal number of change-points and their location such that the results can be found in figure (4).

Starting again by the upper left panel in a clockwise manner, the first plot indicates how the algorithm succeeds in capturing the presence of the change-point for the mean cumulative function  $m(t|\theta)$ ; as the previous two settings before the change-point  $\tau_1 = 825$  the values taken by the function grow in a steady smooth manner until the presence of the instant where the break or rupture is experienced. After such break  $m(t|\theta)$  take larger values which is consistent with the behavior of the simulated data.

On the other hand, according to the next plot (upper right panel) the minimum reached for the Bayesian-MDL was found around the 50th generation taking a value close to 800; such generation is marked explicitly in the lower right panel by the vertical dashed line while the optimal number of change-points detected was  $J = 3$  as per the horizontal dashed line.

Despite the real value of  $J = 1$  being different to the estimated one, in the last panel (lower left) the bar associated with the more frequent change-point can be found in a neighborhood of  $\tau_1 = 825$  of six values before and after such instant;

then, in this interval in 50% of the times it can be found the real value of such  $\tau_1$ .

#### 4.1.2 Two Change-points

##### First Setting

The first setting corresponds to the change-points  $\tau_1 = 275$  and  $\tau_2 = 821$ . As in the three previous cases again, the genetic algorithm was ran and according to the values that optimize the Bayesian-MDL the mean cumulative function was fitted and as well the estimates for the number of change-points and their location. This results are presented in figure (5).

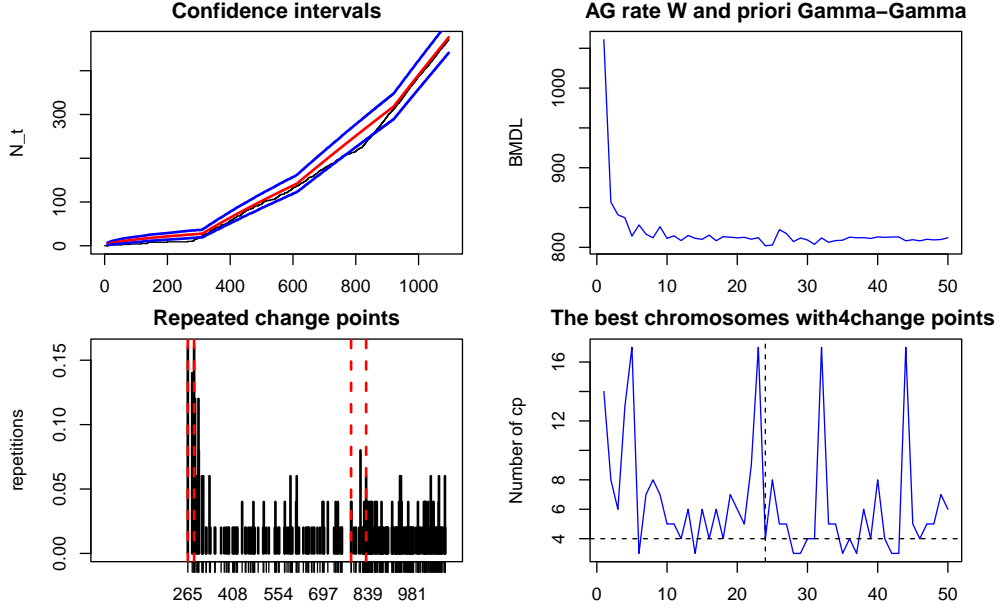


Figure 5: Genetic algorithm results - 2 change-points, first setting

Beginning with the plot in the upper left panel and in a clockwise manner, in contrast to the cases where one change-point was located here two breaks can be appreciated for the values taken by the mean cumulative function  $m(t|\theta)$ . The first breaks occurs around the first change-point  $\tau_1 = 275$  such that for  $0 < t < 275$ ,  $m(t|\theta)$  grows in a steady manner; after said time a change is experienced in the function with its values being larger than the previous regime. While there exist some irregularities the behavior continues to be steadily increasing and captured by the estimate of  $m(t|\theta)$  and the confidence interval at 95%. A second break is experienced then around the second change-point  $\tau_2 = 821$  with the last increase in the values of  $m(t|\theta)$  experienced until the end of the series.

In the second plot (upper right panel) we can observe again the evolution of the Bayesian-MDL with respect to the generations of the genetic algorithm. The optimal value found by said algorithm was found to be just more than 800 and as noted through the vertical dashed line in the third plot (lower right panel) such optimum was reached around the 25th generation. This plot as well indicates the optimal number of change-points with the horizontal dashed-line such that  $J$  was equal to 3.

On the other hand, while the real value of  $J$  was equal to 2, yet, most of the change-points detected clustered around the real values of  $\tau_1$  and  $\tau_2$  according to the last plot (lower left panel). Taking in both cases a neighborhood of six change-points before and after the real  $\tau_i$ ,  $i = 1, 2$  in around 50% of the generations these can be found in such intervals.

##### Second Setting

Now, we have the case where  $\tau_1 = 547$  and  $\tau_2 = 823$ . Proceeding as in the previous cases we have the results presented in figure (6). We start again by the upper left panel in a clockwise manner where we have the mean cumulative function

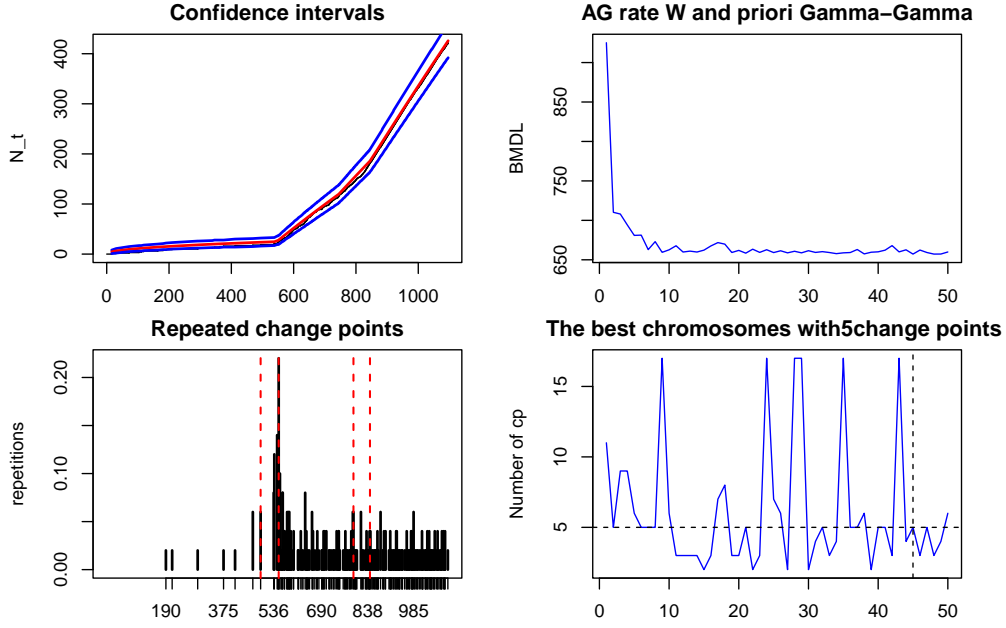


Figure 6: Genetic algorithm results - 2 change-points, second setting

$m(t|\theta)$  estimated through the values found optimal by the Bayesian-MDL.

Here for approximately  $0 < t < 547$ ,  $m(t|\theta)$  grows in a steady manner such that when we get closer to the first change-point it can be appreciated as well, the first break in the values of the function which are fitted in a precise way. After such instant, the values of  $m(t|\theta)$  are also larger in comparison than those of the previous regime and continue to grow despite some small irregularities which could be considered negligible in regards of the next break which is more notorious for the mean cumulative function as we approach to  $\tau_2$ . From this point on, the mean cumulative function is in its last regime and the values it takes are the highest until the end of the time window. Throughout its path, the algorithm correctly adjusts the cumulative mean function and even more so, the 95% confidence intervals found are narrow and contain all its values.

We follow next to analyze the evolution of the Bayesian-MDL in terms of each generation of the genetic algorithm (upper right panel) such that the optimal value detected by the search method was slightly larger than 650 and was found according to the vertical dashed line in the third plot (lower right panel) close to the 45th generation. Likewise, the third plot indicates through the dashed horizontal line the number of change-points detected as optimal which was  $J = 5$ .

While the genetic algorithm differs in the estimate of the real value of  $J$ , most of the change-points found cluster around the real values of  $\tau_i$ ,  $i = 1, 2$  as observed in the last panel (lower left) of the figure (6). Again we took a neighborhood of six points detected before and after  $\tau_1$  and also for  $\tau_2$  such that said intervals combined contain in around 50% of the times the values of interest, that is,  $\tau_1 = 547$  and  $\tau_2 = 823$ .

### Third Setting

Now to end the case of two change-points we have the setting  $\tau_1 = 365$  and  $\tau_2 = 730$  with the results of the implementation of the genetic algorithm presented in the figure (7). We start by analyzing the fitting of the mean cumulative function (upper left panel) and move in a clockwise manner.

In the first plot the fit of  $m(t|\theta)$  is presented (middle solid red line) such that its values overlap with the real ones (middle solid black line) while the upper and lower lines (in blue) correspond to the 95% confidence intervals for the estimate of the mean cumulative function. Again, as in the previous cases such estimates grows in a piecewise manner following the behavior of the real values with breaks defined by the change-points.



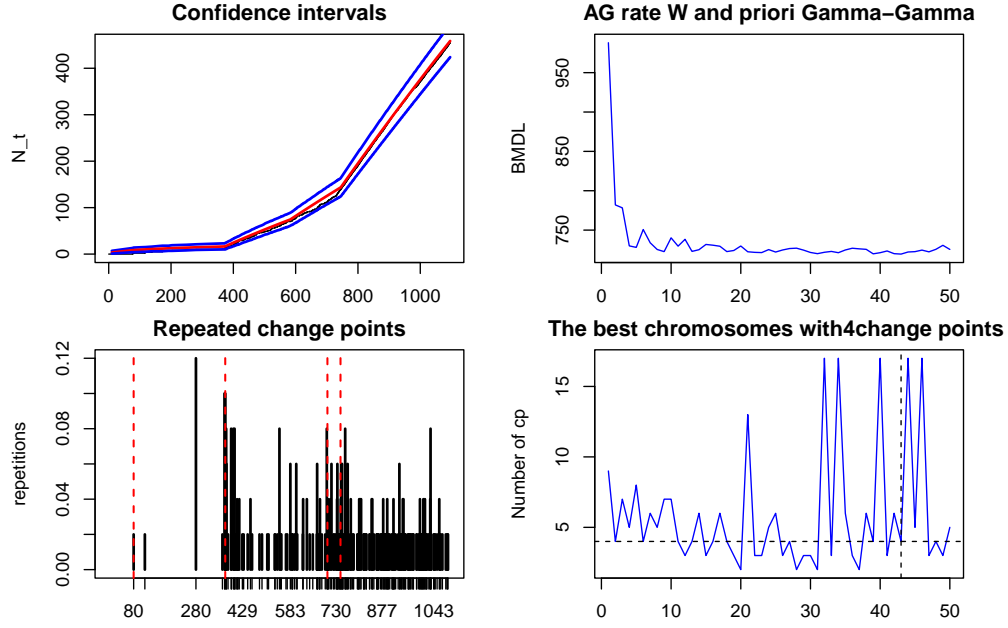


Figure 7: Genetic algorithm results - 2 change-points, third setting

Thus, the first regime for  $m(t|\theta)$  is defined for the times  $0 < t < 365$  approximately such that from the first time the function grows in a steady monotonous manner before experiencing local maximum around time 365; then a similar growth is experienced from around the time 365 until the second change-point  $\tau_2$ . Then we find the next regime which goes from  $\tau_2 = 549$  until the third change-point  $\tau_3 = 823$  and finally we have the fourth regime which goes from the previously mentioned instant until the end of the time window.

Next we have the evolution of the Bayesian-MDL in terms of each generation of the genetic algorithm (upper right panel). Here the algorithm detects as the optimum for said function a value of around 750; such value is reached according to the vertical dashed line in the third plot (lower right panel) around the 43rd generation.

The genetic algorithm estimated  $J = 4$  according to the horizontal dashed line in the third plot, being its real value  $J = 2$ ; nevertheless as can be seen in the last plot (lower left panel) the detected change-points cluster around the real values of  $\tau_1$  and  $\tau_2$ . Again we define a neighborhood for both change-points and while for the first one its length was larger, both intervals contain in around 50% of the times the real values of the  $\tau_i$ ,  $i = 1, 2$ .

#### 4.1.3 Three Change-points

##### First Setting

Now we have the case of three change-points. We start with the setting where  $\tau_1 = 275$ ,  $\tau_2 = 549$  and  $\tau_3 = 823$  and the results are presented in the figure (8). We begin by analyzing the plot in the upper left panel and then we follow in a clockwise manner for the others.

Thus, we have in the first place the estimate of the mean cumulative function  $m(t|\theta)$  when there are three change-points. Again it can be appreciated how the genetic algorithm allows for the capture of the behavior of the values of  $m(t|\theta)$  where it does fit them in a precise manner for all the series path as much as for the mean and as for the 95% confidence intervals. Again there are instants where the mean cumulative function exhibits some breaks as in previous cases which are associated to the presence of the change-points. The first break contains approximately the values for  $0 < t < 275$  such that in the interval there is a steady growth until we reach the first time of interest. After said time, there is also a monotonous growth until the second change-point is reached,  $\tau_2 = 549$ . Next there is an uniform growth with some negligible irregularities until the end of the time window is reached; although the presence of the third change point is not so marked, even so, near the associated instant, its influence on the behavior of the cumulative mean function can be

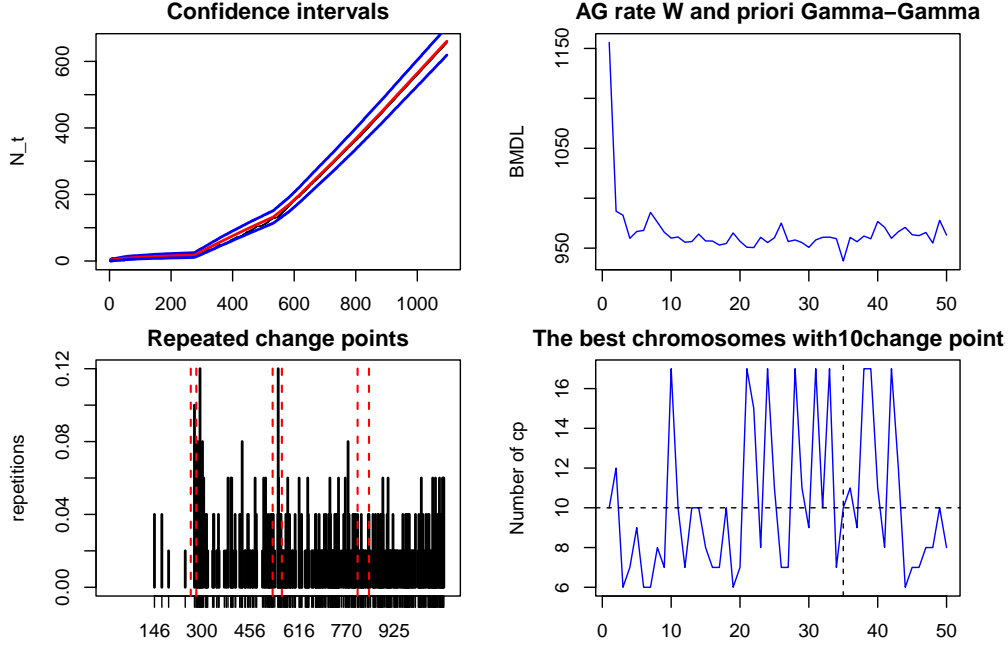


Figure 8: Genetic algorithm results - 3 change-points, first setting

appreciated and captured as well by the genetic algorithm.

Then we have the evolution of the Bayesian-MDL in terms of the generations of the genetic algorithm such that the minimum is close to 937.13 and it is reached according to the vertical dashed line in the third plot (lower right panel) around the generation 35. On the other hand, the third plot as well, shows the number of change-points detected as optimal which in this case, corresponds to  $J = 10$  while its real value was  $J = 3$ .

However, in the last plot again (lower left panel), the behavior of the detected change-points indicates that these cluster around the real values of  $\tau_i$ ,  $i = 1, 2, 3$ . Furthermore for each  $\tau_i$ ,  $i = 1, 2, 3$ , the defined intervals (vertical dashed lines) correspond to a neighborhood of six change-points before and after such that when combined these three, around 50% of the times they contain the real values of the instants of interest.

### Second Setting

Here we have the case of three change-points located at positions  $\tau_1 = 548$ ,  $\tau_2 = 823$  and  $\tau_3 = 973$  and as well, the results of executing the genetic algorithm under the presence of such instants which are presented in the figure (9).

We begin by analyzing the plot in the upper left panel which corresponds to the mean cumulative function  $m(t|\theta)$  such that its fitted values are precisely estimated (middle red line), even more so, these overlap with the true values (middle black line) as well as the confidence intervals at 95% (upper and lower blue lines). For the time interval  $0 < t < 548$  approximately we found the first regime estimated by the genetic algorithm which remains constant and monotonous; after the mentioned time we found the following regime bounded by the first and second change-points and finally, we have the last regime which goes from the second change point,  $\tau_2 = 823$  until around the time 1096 where the last increase in the values of  $m(t|\theta)$  is experienced. While the last change-point seems not present for the mean cumulative function, the genetic algorithm succeeds in capturing most of its behavior.

Then we move to the second plot in a clockwise manner (upper right panel) which corresponds to the evolution of the Bayesian-MDL in terms of the generations of the genetic algorithm. Here we can appreciate that the value taken by the objective function as optimal is reached around 575 and according to the vertical dashed line in the third plot (lower right panel), such value was found in the 48th generation. Likewise, the third plot gives us the number of change-points

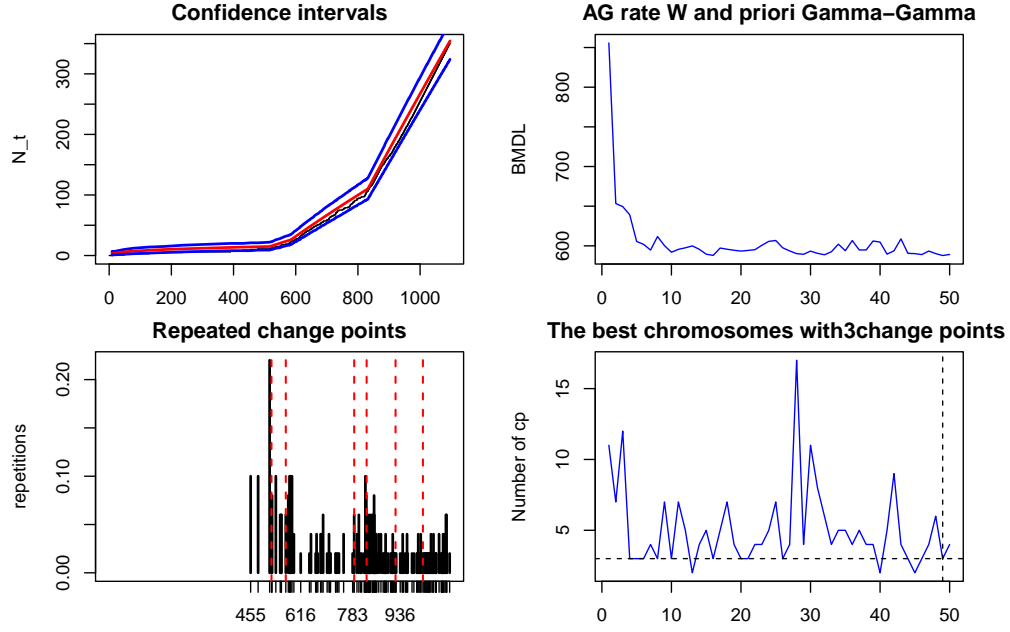


Figure 9: Genetic algorithm results - 3 change-points, second setting

which optimize the Bayesian-MDL which was of  $J = 3$ , the real value of  $J$ .

Finally we have the last plot (lower left panel) where a similar behavior to the previous cases is experienced for the estimated change-points such that for the 50 generations these values cluster around the real ones  $\tau_i$ ,  $i = 1, 2, 3$ . Furthermore, here, the neighborhoods of six change-points before and after the real values were narrow and combined, in 50% of the times those instants were found inside the intervals.

### Third Setting

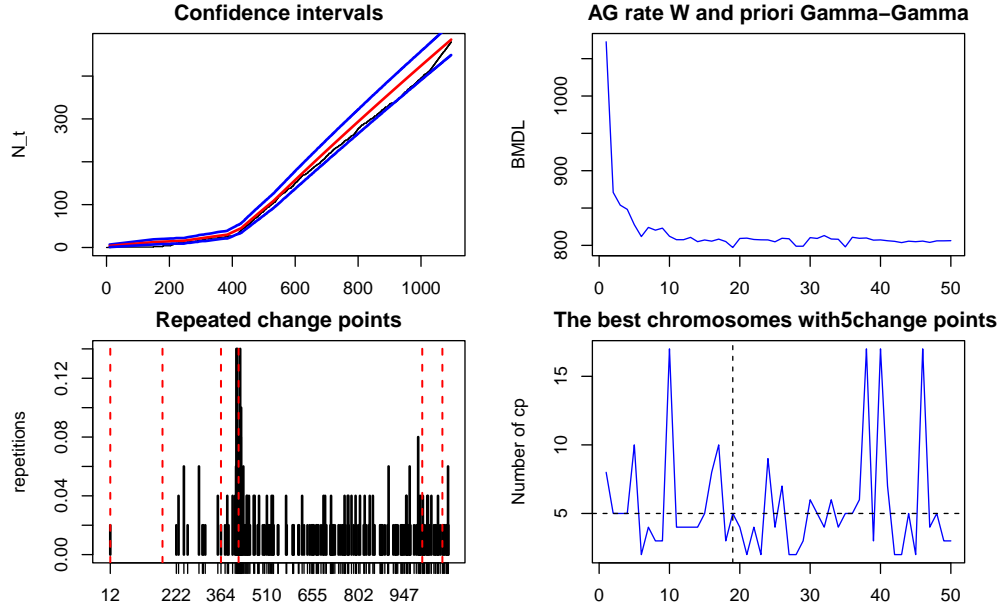


Figure 10: Genetic algorithm results - 3 change-points, third setting

Finally we have now the case of three change-points located at  $\tau_1 = 169$ ,  $\tau_2 = 413$  and  $\tau_3 = 1027$  such that the results of applying the genetic algorithm are presented in figure (10).

Beginning with the analysis of the mean cumulative function (upper left panel), the algorithm captures the behavior of the real values of  $m(t|\theta)$  such that for all the path of the series the estimates of the function (middle red line) overlap with the real values and the confidence interval at 95% (upper and lower blue lines) captures the fitted values and the real ones. As in the other cases there are breaks in the mean cumulative function, nevertheless, here the only break is associated to the second change-point,  $\tau_2 = 413$  such that the other possible ruptures can barely be seen.

Now we analyze how does the Bayesian-MDL evolves according to the generations of the genetic algorithm (upper right panel) such that its behavior seems to be approximately constant for all its path with some decreases such that the optimal value was found to be around 797.16. Said optimum was reached in generation 25 as noted by the vertical dashed line in the third plot (lower right panel); on the other hand, the optimal number of change-points was found to be  $J = 5$  according to the horizontal dashed line in the third panel.

Again, while there the real value of  $J$  is equal to 3, nevertheless as in the previous cases the estimated change-points (lower left panel) cluster around the real ones. Furthermore, except for the first change-point, when we defined a neighborhood for said instants in around 50% of the time they were found in the intervals. Now we proceed to analyze how does the algorithm behaves for the real data.

## 4.2 Real Data Analysis

Here we applied on the  $PM_{2.5}$  series for Bogotá in the period 2018 - 2020, in an exhaustive manner the genetic algorithm with the already described settings at the beginning of this section and using as well as an objective function (21). As threshold, the one established by the environmental norm for Colombia was used which specifies that presence of this polluting agent can not overpass  $37\mu g/m^3$ . The series can be observed in figure (11) where different exceedances from the norm are over the horizontal dashed line.

Then, the optimal chromosome was found to be (8, 400, 408, 445, 488, 627, 654, 661, 798), such that there are  $J = 8$  change-points according to the horizontal dashed line in the third plot (lower right panel) of figure (12); next the respective location for these points in the 1096 days of the observed timeline are given, it can be observed as well, that the first 4 change-points are very close such that the intervals (vertical dashed lines) overlap in most of cases. The table (3) shows the date corresponding to each change-point.

Change Point	Day of the week	Date
400	Monday	February 4, 2019
408	Tuesday	February 12, 2019
445	Thursday	March 21, 2019
488	Friday	May 3, 2019
627	Thursday	September 19, 2019
654	Wednesday	October 16, 2019
661	Wednesday	October 23, 2019
798	Sunday	March 8, 2020

Table 3: Points of change with their respective dates

These surpasses occurred during the rainy season in Bogotá. If the dates in the table above are compared with the measurements in figure (11), the seasons with the most consistent peaks over time can be captured.

As can be seen in the other plots in figure (12), the one in the upper left panel shows the adjustment of the cumulative mean function  $m(t|\theta)$  (black line) by means of the point averages, obtained from the vectors of parameters better qualified by the MDL (red line), and their respective 95% confidence intervals (blue lines).

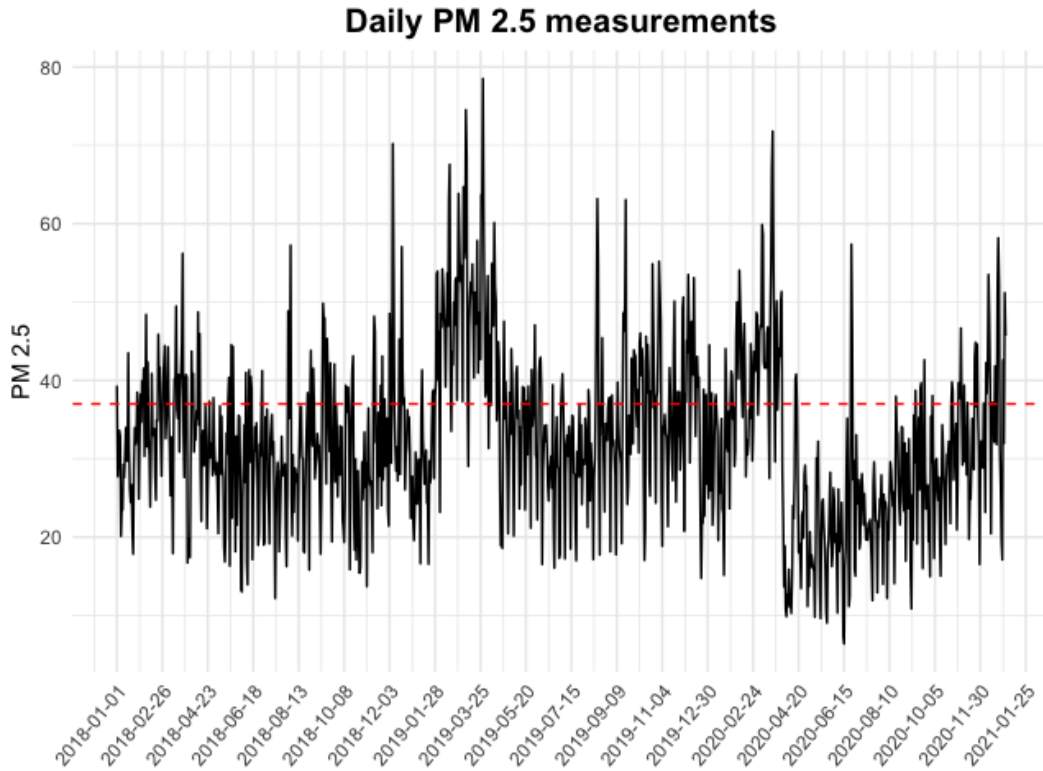


Figure 11:  $PM_{2.5}$  Measurements in Bogota, January 1 2018 - December 21 2020

Also, the corresponding optimal Bayesian-MDL was 778.44 as per the upper right panel which shows the evaluation of said metric for each one of the best chromosomes of each of the 45 generations such that the minimum is reached around the 45th one (vertical dashed line in the lower right panel).

Finally, in the lower left panel, the histogram shows the days in the time series that exceed the threshold, which appear most frequently in the first 50 chromosomes of the 50 generations analyzed.

The graph in figure (13) shows that before day 400, i.e., Monday, February 4, the rate of exceedances of the  $37 \mu\text{g}/\text{m}^3$  threshold had been decreasing sharply, but after it, the highest emission rate for eight consecutive days was recorded. This high average rate is around 1.004, as shown in (Table4) for the second regime. In the third regime, it decreased to an average rate of 0.9468; in the fourth, it jumps to 0.6748, and it is in the fifth regime that it achieves the lowest drop, 0.2090, before the intensity function rises again to levels above the 0.2 threshold overshoots per unit of time. This rate present in the fifth regime goes from May 3 to September 19, 2019. Thus, it is evident that the fifth regime occurred before the COVID-19 pandemic lockdown was declared in Colombia. Therefore, this may be the result of a public policy aimed at reducing the emissions of  $PM_{2.5}$ .

As part of the 2010-2020 ten-year plan for air pollution control, the use of emission control systems in cargo transport vehicles and motorcycles, and as well as the integrated public transport system (SITP for its acronym in Spanish) policies were implemented. The later includes the replacement of old buses with internal combustion engine with electric or hybrid buses. In addition to the above, a few days before the fifth regime, resolution 383 (see RES19 (2019)) was issued, which declared a yellow alert for particulate matter exceedances. Considering the first regime represented in figure (13), the rapid deceleration in the emission of threshold exceedances can also be seen as a consequence of this resolution. Such is the case of restrictions on the use of transportation and the mobility sector, in addition to those aimed at the operations of industries that use combustion processes associated mainly with the burning of biomass and the use of fossil or liquid fuels.

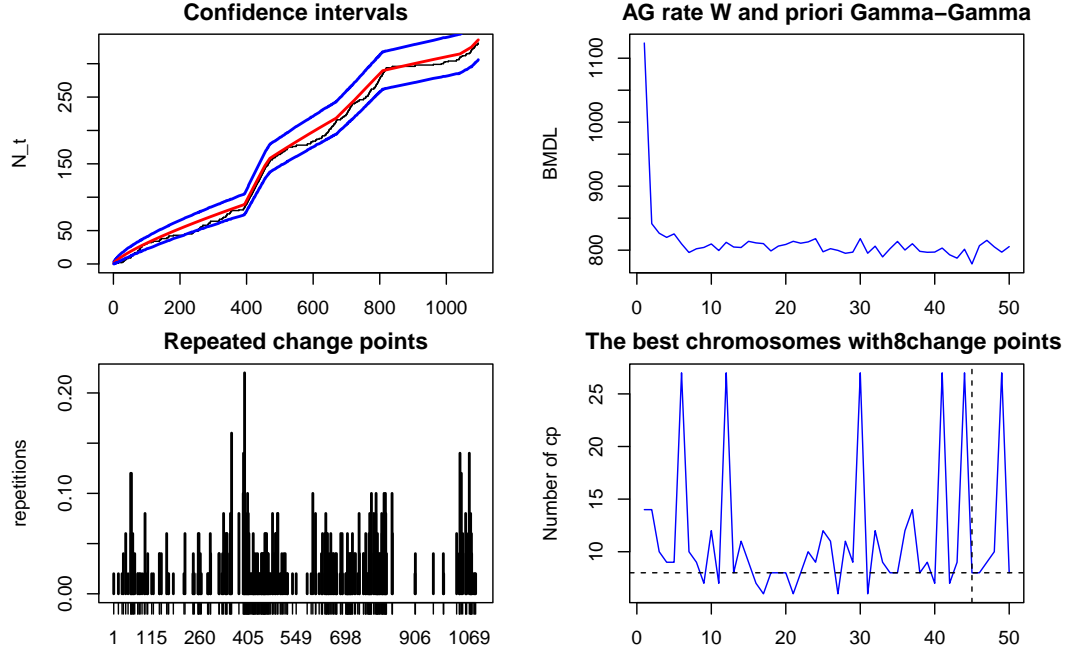


Figure 12: Results for the Optimal Chromosome

Regime	Min	Mean	Max
1	0.1894	0.2379	0.6555
2	1.002	1.004	1.007
3	0.9363	0.9468	0.9577
4	0.6657	0.6748	0.6841
5	0.1991	0.2090	0.2201
6	0.4801	0.4832	0.4864
7	0.5765	0.5773	0.5781
8	0.4761	0.4896	0.5043
9	0.1744	0.1849	0.1971

Table 4: Minimum, Maximum and Mean for each Regime

## 5 Conclusions and future work

A solution has been presented to determine change points in counting time series, particularly when they exceed an environmental standard of interest. So, the need for specifying a likelihood function was overpassed by modeling the times of the series where existed exceedances through a non-homogeneous Poisson process and this specification allowed for better estimations of the number of change-points with a lower variability and a better estimation of parameters of the underlying generating process.

A family of such objective functions was derived using different definitions for the mean cumulative function of the non-homogeneous Poisson processes but it is yet to be seen the influence of using one or the other on the estimation of the change-points and their location.

The search method for the change-points was a genetic algorithm similar to the one exposed by [5], nevertheless, there is still room for improvement for it in terms of different operators available at literature and as well the use of other families of such algorithms.

The detection of change-points using a genetic algorithm and a Bayesian-MDL as selection criterion yielded results that agree with the public policies implemented in Bogotá, Colombia, both regarding the contamination alerts issued by

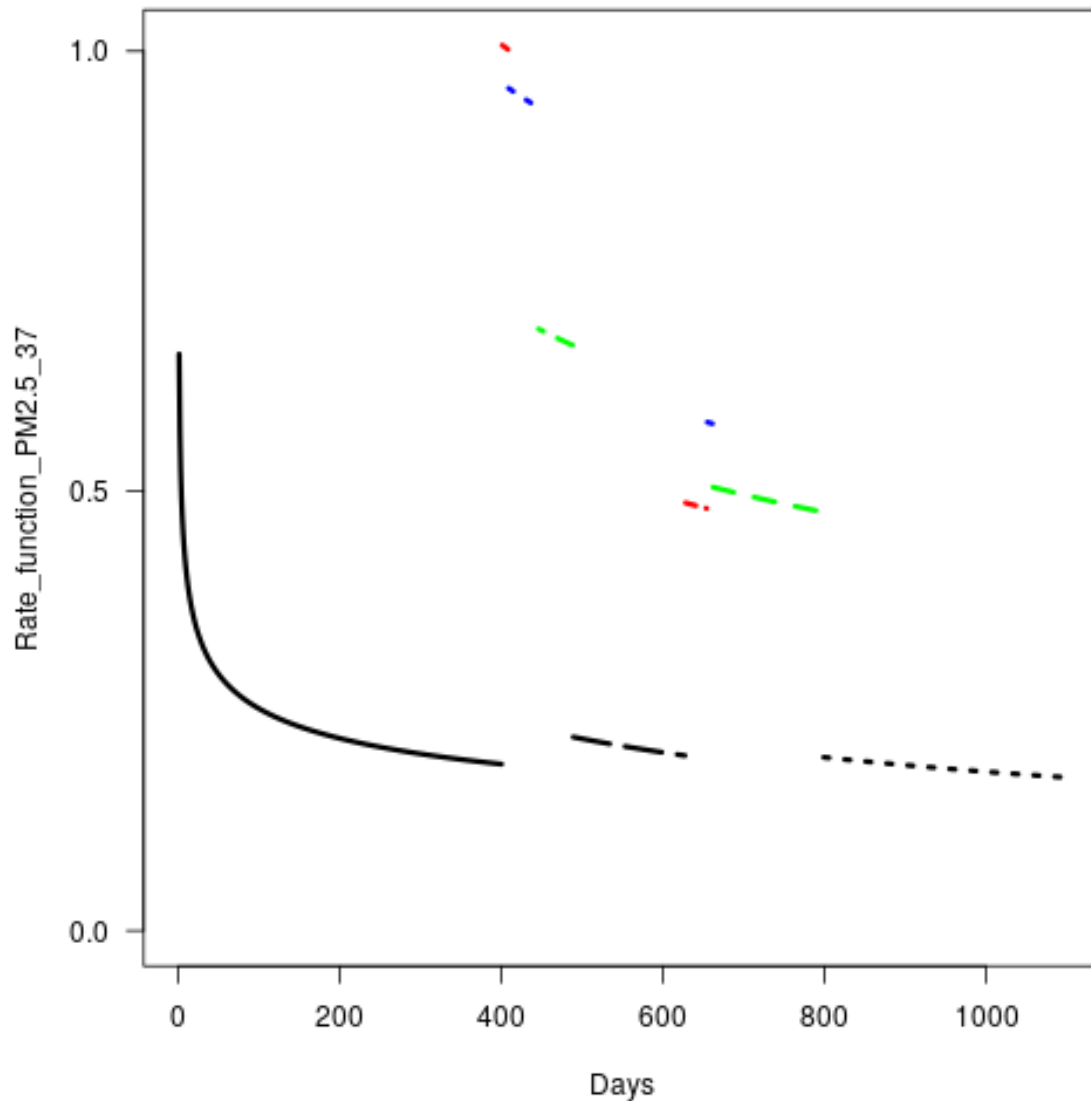


Figure 13: Rate function for  $PM_{2.5}$  by Days

the monitoring network, as well as the mobility restrictions due to the quarantine caused by the SARS-CoV-2 virus pandemic.

The good performance of the algorithm is partly due to the fact that in [18] and [17], the cumulative means function of the contamination exceedances was adjusted, but by then there was no computational technique for the automatic detection of change-points.

We hope that in the near future these methods will prove to be a useful tool for the government agencies in charge of measuring the effectiveness of the actions taken to reduce air pollution, and thus reduce its impacts both in the environment and the health of the inhabitants.

## References

- [1] Michèle Basseville and Igor V. Nikiforov. *Detection of Abrupt Changes - Theory and Application*. Prentice Hall, Englewood Cliffs, NJ, 1993.

- [2] Charles Truong, Laurent Oudre, and Nicolas Vayatis. Selective review of offline change point detection methods. *Signal Processing*, 167:107299, 2020.
- [3] Samaneh Aminikhanghahi and Diane Cook. A survey of methods for time series change point detection. *Knowledge and Information Systems*, 51:339–367, 2017.
- [4] Toby Hocking, Guillem Rigai, and Guillaume Bourque. Peakseg: constrained optimal segmentation and supervised penalty learning for peak detection in count data. In Francis Bach and David Blei, editors, *Proceedings of the 32nd International Conference on Machine Learning*, volume 37 of *Proceedings of Machine Learning Research*, pages 324–332. PMLR, 2015.
- [5] Shanghong Li, Robert Lund, Li, and Robert Lund. Multiple Changepoint Detection via Genetic Algorithms. *Journal of Climate*, 25(2):674–686, jan 2012.
- [6] J. Achcar, A. Fernandez-Bremauntz, E. Rodrigues, and G. Tzintzun. Estimating the number of ozone peaks in mexico city using a non-homogeneous poisson model. *Environmetrics*, 19:469–485, 2008.
- [7] B. Suarez-Sierra, E. Rodrigues, and G. Tzintzun. Rate of ozone and pm10 exceedances: A case study comparing data from mexico city and bogota. *Communications in Statistics: Case Studies, Data Analysis and Applications*, 5(2):153–165, 2019.
- [8] B. Suarez-Sierra, E. Rodrigues, and G. Tzintzun. An application of a non-homogeneous poisson model to study pm2.5 exceedances in mexico city and bogota. *Journal of Applied Statistics*, 49(9):2430–2445, 2022.
- [9] J. F. Lawless. *Statistical Models and Methods for Lifetime Data, Second Edition*. John Wiley and Sons, Inc., Hoboken, NJ, 2 edition, 2002.
- [10] D. R. Cox and P. A. W. Lewis. *The statistical analysis of series of events*. Methuen’s Monographs on Applied Probability and Statistics. Springer Dordrecht, 1 edition, 1966.
- [11] G. S. Mudholkar, D. K. Srivastava, and M. Freimer. The exponentiated weibull family: A reanalysis of the bus-motor-failure data. *Technometrics*, 37(4):436–445, 1995.
- [12] Cid Ramirez, Juan Esteban, and Jorge Alberto Achcar. Bayesian inference for nonhomogeneous poisson processes in software reliability models assuming nonmonotonic intensity functions. *Computational Statistics & Data Analysis*, 32(2):147–159, December 1999.
- [13] J. D. Musa and K. Okumoto. A logarithmic poisson execution time model for software reliability measurement. In *Proceedings of the 7th International Conference on Software Engineering*, ICSE ’84, pages 230–238, Piscataway, NJ, USA, 1984. IEEE Press.
- [14] Amrit L. Goel and Kazu Okumoto. An analysis of recurrent software errors in a real-time control system. In *Proceedings of the 1978 Annual Conference*, ACM ’78, pages 496–501, New York, NY, USA, 1978. ACM.
- [15] E. R. Rodrigues and J. Achcar. *Applications of Discrete-time Markov Chains and Poisson Processes to Air Pollution Modeling and Studies*. Number 1 in SpringerBriefs in Mathematics. Springer-Verlag New York, 2013.
- [16] Bo-Yi Yang, Shujun Fan, and E. Thiering. Ambient air pollution and diabetes: A systematic review and meta-analysis. *Environmental Research*, 180, 2020.
- [17] J. Achcar, E. Rodrigues, and G. Tzintzun. Using non-homogeneous poisson models with multiple change-points to estimate the number of ozone exceedances in mexico city. *Environmental and Ecological Statistics*, 22, 2011.
- [18] J.A. Achcar, E. Rodrigues, C. Paulino, and P. Soares. Non-homogeneous poisson processes with a change-point: an application to ozone exceedances in México city. *Environmental and Ecological Statistics*, 17:521–541, 2010.
- [19] Richard A Davis, Thomas C. M Lee, and Gabriel A Rodriguez-Yam. Structural Break Estimation for Nonstationary Time Series Models. *Journal of the American Statistical Association*, 101(473):223–239, mar 2006.
- [20] R Core Team. *R: A Language and Environment for Statistical Computing*. R Foundation for Statistical Computing, Vienna, Austria, 2022.
- [21] Marie Laure Delignette-Muller and Christophe Dutang. fitdistrplus: An R package for fitting distributions. *Journal of Statistical Software*, 64(4):1–34, 2015.
- [22] Brian Rumburg, Richard Alldredge, and Candis Claiborn. Statistical distributions of particulate matter and the error associated with sampling frequency. *Atmospheric Environment*, 35(16):2907–2920, 2001.